Proceedings of the
International Conference on Mechanical Engineering 2003
(ICME2003) 26- 28 December 2003, Dhaka, Bangladesh

ICME03-TH-18

OPTIMIZATION OF ROCKET BASED COMBINED CYCLE (RBCC) ENGINE

Nayem Jahingir[1], Ziaul Huque[2] and Shaheen I Alam[1]

CFD Institute
Department of Mechanical Engineering
Prairie View A & M University
Prairie View, TX.

ABSTRACT

The objective of the current study was to optimize the inlet/ejector system of a Rocket Based Combined Cycle (RBCC) Engine. For this purposes, a two-dimensional rocket-ejector system was studied over a matrix of engine design variables. The engine design variables that defined the trade space were: by pass ratio, ejector compression ratio and ejector/mixture thrust efficiency. The computational fluid dynamics (CFD) simulations of the inlet/ejector system were carried out with Finite Difference Navier Stokes (FDNS) code. The Gaseous O_2/H_2 combustion physics were solved finite rate with a system of seven species and nine reactions. The desirability approach of optimization, tied with response surface and neural networks technique has been used for response surface generation and inlet/ejector optimization. An optimum primary thruster size, duct length-to-diameter ratio and ramjet burner to ejector/mixer inlet area ratio are obtained.

Keywords: CFD, Optimization, Response Surface, RBCC

1. INTRODUCTION

A major goal driving current space propulsion research is to significantly decrease the cost of access to space. There are currently efforts underway to develop reusable launch vehicles that promise to decrease long-term costs as compared to the traditional expendable staged vehicles. One way to use high-efficiency air breathing cycles during ascent in a reusable system is through the use of combined-cycle propulsion (CCP) systems. CCP systems can be broadly divided into two categories: air breathing combined-cycles and combined cycle systems which include a rocket sub-system. Air breathing combined cycle engines are intended primarily for missions involving high–speed cruises in the atmosphere, but are not candidates for trans-atmospheric flight.

There are many types and variations of CCP systems; one class of rocket-based CCP systems shows promise for Earth-to-orbit (ETO) missions. These are engines that operate in rocket-ejector mode and also have the capability of operating in ramjet, scramjet, and rocket-only modes, and are typically referred to as rocket-based combined-cycle (RBCC) engines. A schematic of a RBCC engine is shown in Figure 1. Many of the advantages of RBCC engines result from certain synergistic benefits that would not occur if the two units operated separately[1]. The ability to utilize the rocket as an ejector increases the thrust. Afterburning in rocket-ejector mode, using the ramjet/scramjet fuel injectors, further increased the thrust and specific impulse compared to the rocket alone. As the ratio of the bypass air to the rocket exhaust increases with increasing flight speed, the specific impulse continues to increase, as the cycle more closely resembles ramjet operation. In ramjet and scramjet modes, the rocket could be advantageously used as a fuel injector and mixing enhancer. In the rocket-only mode, the use of the engine duct as a highly expanded nozzle at high altitudes increases the specific impulse of that mode of operation. Another key advantages of RBCC systems is the reduction in the amount of onboard oxidizer required. This decreases the size and, therefore, the weight, of the tank and vehicle[1].

An integrated inlet/ejector is one of the most critical parts of a RBCC engine propulsion system. Its design must be such that it delivers air to the engine at the desired mass flow rate and flow conditions for all flight Mach numbers. This delivery must be accompanied by as little losses, drag, weight, and complexity as possible. In short, the design is a trade-off or compromise between a high-pressure recovery and low drag. This compromise can only be found after several propulsion and vehicle performance calculations, which strongly depends on the mission of the vehicle.

1 Graduate Research Assistant
2 Associate Professor

The objective of this study was to optimize the inlet/ejector system of a RBCC engine. For this purposes, a two-dimensional rocket-ejector system was studied over a matrix of engine design variables. The engine design variables that defined the trade space were: ejector/mixer aspect ratio, L/D; the ratio of secondary to primary flow areas, A_s/A_p and ratio of ramjet burner to ejector/mixer inlet areas, A_8/A_5. Figure 1 defines some of the RBCC engine design variables. Each variable had three values so that the initial trade space was 27 configurations as shown in table 1. A 28th configuration was run to explore the effect of a constant area mixer (A_8/A_5=1.0). The performance of the ejector/mixer was measured with the following figures of merit (FOM): by-pass ratio, the ratio of secondary flow to primary flow; ejector compression ratio (ECR), the ratio of total pressure at ejector/mixer exit to total pressure of secondary flow and ejector/mixer thrust (nozzle) efficiency, thrust at the exit divided by thrust at the mixer inlet. Primary thruster mass flow rates were kept constant for all configurations but each A_s/A_p ratio resulted in a different primary thruster area ratio, therefore, a different primary thruster exit pressure. The primary thruster exit flow properties were calculated with the Reacting and Multiphase Program.

2. APPROACHES

2.1.1 CFD Simulation

The RBCC flow path configuration for this analysis was 2-D with a single primary thruster on the engine centerline. The primary thruster was housed in a center body that created an annular constant area inlet. The Inlet/Ejector plane is defined to be the exit plane of the primary thruster. The secondary inlet length (L) was a function of two of the trade space variables, L/D and A_s/A_p. A_s is the area of the secondary flow area at the mixer inlet plane and A_p is the area of the primary thruster exit area plus any base area surrounding the thruster. A_5 is the total flow area at the ejector/mixer inlet plane ($A_s + A_p$) and A_8 is the flow area of the ramjet burner. The engine design variables that defined the trade space were: secondary inlet aspect ratio L/D; A_s/A_p, the ratio of secondary to primary flow areas; and A_8/A_5, ratio of ramjet burner to ejector/mixer inlet areas. The engine design trade space is shown in Table 1.

The CFD simulation of the RBCC internal flow path was performed with FDNS. The code solves the Reynolds-averaged transport equations with a variety of options for physical models and boundary conditions. A pressure-based predictor plus multiple-corrector solution method is employed so that flow over a wide speed range (from low subsonic to supersonic) can be analyzed. The present analysis was solved steady state, implementing the third order TVD scheme and an extended two-equation turbulence model with compressibility correction. The GO_2/GH_2 combustion physics are solved as a system of seven species and nine reactions.[11]

2.1.2 Grid Description

To obtain a grid independent solution several grid density pararnetrics was performed. The computational domain consists of a 2-D representation of the experimental hardware internal flow path. The structured grid had approximately 15000 nodes in 15 zones. Non-matching zonal boundaries were implemented at several locations to keep the number of nodes from becoming excessive. The geometric definition of the 27 configurations was provided by an engine design spreadsheet. All grids contained the same number of nodes in the freestream, inlet, ram burner and nozzle portions of the domain. The number of nodes in the axial direction of the ejector/mixer varied because of their different lengths. A consistent axial delta-s was used in the ejector/mixer region. The blockage created by the rocket engine was modeled in the flow path; however, the rocket engine's internal flow path was not contained in the present computational domain.

The considered analysis geometry of RBCC engine has two inlet bound The CFD simulation of the RBCC internal flow path was performed with FDNS. The code solves the Reynolds-averaged transport equations with a variety of options for physical models and boundary conditions. A pressure-based predictor plus multiple-corrector solution method is employed so that flow over a wide speed range (from low subsonic to supersonic) can be analyzed. The present analysis was solved steady state, implementing the third order TVD scheme and an extended two-equation turbulence model with compressibility correction. The GO_2/GH_2 combustion physics are solved as a system of seven species and nine reactions.[11]

2.1.2 Grid Description

To obtain a grid independent solution several grid density pararnetrics were performed. The computational domain consists of a 2-D representation of the experimental hardware internal flow path. The structured grid had approximately 15000 nodes in 15 zones. Non-matching zonal boundaries were implemented at several locations to keep the number of nodes from becoming excessive. The geometric definition of the 27 configurations was provided by an engine design spreadsheet. All grids contained the same number of nodes in the freestream, inlet, ram burner and nozzle portions of the domain. The number of nodes in the axial direction of the ejector/mixer varied because of their different lengths. A consistent axial delta-s was used in the ejector/mixer region. The blockage created by the rocket engine was modeled in the flow path; however, the rocket engine's internal flow path was not contained in the present computational domain.

2.1.3 Boundary Conditions

The considered analysis geometry of RBCC engine has two inlet boundaries. One is for secondary air inlet and the other one is for primary thruster inlet. In real practice primary thruster was built as an integral part of the RBCC engine system but for computational benefit the rocket engine's flow computation was performed separately.

Primary Thruster Simulation: A 1-D rocket simulator code for calculation of complex chemical equilibrium compositions and applications (CEA)[12] was used to calculate the rocket exit properties for different primary thruster area ratio. For this analysis primary

thruster size was varied to justify the amount of secondary air entrainment. This GO_2/GH_2 primary rocket was designed to operate at an operation pressure of 3.45 MPa with oxygen to fuel (O/F) ratio 4.0. The three different A_s/A_p ratio resulted three different supersonic area ratio, which drastically change the rocket outlet conditions. Table 2 summarizes the results of individual rocket analysis with chemical equilibrium code for three different design conditions. These thruster exit flow properties were defined as fixed inlet conditions for the ejector/mixer analysis.

Inflow, Outflow and Engine Surface Boundaries: In the computational model the secondary inlet was specified as subsonic, fixed total conditions boundary. In this boundary the values of two dependent flow-field variables were stipulated, whereas the value of other variable allowed to float. The rocket nozzle exit condition was supersonic and used as fixed inlet conditions for the RBCC engine analysis. All engine surfaces were set to no-slip adiabatic walls and the centerline of the engine was set to symmetric boundary condition. The zones downstream of the nozzle had a far-field boundary condition applied that maintained one atmosphere pressure on the boundary. The right-most face was set as an exit boundary.

2.1.4 Combustion Modeling

In a conventional ejector-ramjet, a fuel-rich rocket exhaust is mixed and burned with air captured by the inlet. The rocket provides all of the fuel needed for combustion with the entrained air. In the considered case the excess GH_2 in the rocket plume depletes the GO_2 in the air stream, there was no downstream introduction of GH_2. The GO_2/GH_2 combustion physics were solved finite rate with a system of seven species and nine reactions using FDNS.

2.2 Neural Network

Neural networks are composed of simple elements operating in parallel. These elements are inspired by biological nervous systems. As in nature, the network function is determined largely by the connections between elements[3]. A neural network (NN) can be trained to perform a particular function by adjusting the values of the connections (weights) between elements. Commonly neural networks are adjusted, or trained, so that a particular input leads to a specific target output. The network is adjusted, based on a comparison of the output and the target, until the network output matches the target. Typically many such input/target pairs are used, in this supervised learning, to train a network. In this study back-propagation neural network was used. Standard back propagation is a gradient descent algorithm. The term back propagation refers to the manner in which the gradient is computed for nonlinear multi-layer networks. Present study used NN to build a response surface from 27 CFD runs of a steady sate flow of an inlet/ejector system and later it was used for evaluating an objective function. The data was entered into the net as [3x1] matrix. In the first layer "tansig" function from MATLAB NN toolbox was used as transfer function in three neurons. In the second layer "purelin" was used in one neuron.

2.3 Optimization Approach

For this study the desirability approach of optimization, tied with response surface and neural networks technique has been used for response surface generation and inlet/ejector optimization. The desirability function approach is one of the most widely used methods in industry for the optimization of multiple response processes. The method allows designer's own priorities on the response values to be built into the optimization procedure. One method of optimizing multiple responses simultaneously is to build a composite response known as the desirability function from the individual responses. It is based on the idea that the "quality" of a product or process that has multiple quality characteristics, with one of them outside of some "desired" limits, is completely unacceptable. The method finds operating conditions $\boldsymbol{x}$ that provide the "most desirable" response values. The method gives designer the freedom to setup his own priorities on the response values to be built into the optimization procedure. Desirability approach of optimization was successfully used in the rocket engine ejector optimization.[13]

In the current study, it is desirable to simultaneously maximize the by pass ratio β, ejector compression ratio ECR and Ejector/mixer thrust (nozzle) efficiency η_t. The first step is to develop desirability function, D for each response. In the case where a response should be maximized, such as β, the desirability takes the form:

$$D_1 = \left(\frac{\beta - A}{C - A}\right)^S$$

Where, C is the target value and *A* is the lowest acceptable value such that $D_1 = 1.0$ for any $\boldsymbol{\beta} > C$ and $\mathbf{D_1}=0$ for $\boldsymbol{\beta}<A$. The power value $\boldsymbol{s}$ is a weighting factor, which is set to 1.0 for this case from the assumption of a linear desirability function. For this case a target value of 4.5 and minimum value of 0.5 was assumed for the by pass ratio.

In the case of maximizing Ejector compression ratio (ECR), the desirability takes the form:

$$D_2 = \left(\frac{ECR - F}{E - F}\right)^t$$

Where, E is the target value and F is the lowest acceptable value such that $\mathbf{D_2 = 1.0}$ for any $\mathbf{ECR > E}$ and $\mathbf{D_2=0}$ for $\mathbf{ECR < F}$. The power value **t** is a weighting factor, which is set to 1.0 for this case from the assumption of a linear desirability function. For this case a target value of 2.0 and minimum value of 1.0 were assumed for ejector compression ratio.

To maximize Ejector/mixer thrust (nozzle) efficiency $\boldsymbol{\eta_t}$, the desirability takes the form:

$$D_3 = \left(\frac{\eta_t - G}{H - G}\right)^u$$

Where, H is the target value and G is the lowest acceptable value such that $\mathbf{D_3 = 1.0}$ for any $\boldsymbol{\eta_t} > \mathbf{H}$ and $\mathbf{D_3=0}$ for $\boldsymbol{\eta_t}<\mathbf{G}$. The power value **u** is a weighting factor, which is set to 1.0 for this case from the assumption of a linear desirability function. For this case a target value of 1.0 and minimum value of 0.1 were assumed for

ejector/mixture thrust efficiency η_t. Choices for A, C, E, F, G and H are chosen according to the designer's priorities or, as in the present study, simply as the boundary values of the domain of **β, ECR** and η_t.

A single composite response is developed which is the geometric mean of the desirability's of individual responses. The composite response is defined as:

$$D = (D_1 * D_2 * D_3 \ldots\ldots\ldots\ldots D_m)^{1/m}$$

Which for the present case is:

$$Minimized \quad D = \left(1/D_1 * 1/D_2 * 1/D_3 \right)^{1/3}$$

Reciprocal of each individual response was considered as the total desirability is subject to minimization. This is then submitted to a nonlinear gradient-based optimizer NPSOL[14] to be minimized. In this analysis there were three design variables, such as X_1 represents the isolator aspect ratio L/D, X_2 represents secondary to primary area ratio A_s/A_p and X_3 represents ram burner to total mixture area ratio A_8/A_5.

The CFD data of 27 cases were used to generate a response surface. This response surface was used for training the neural network and later it was used for objective function evaluation, during the optimization process. The optimization was done for a simple bounded from, in which the objective function is both subject to the domain variables and linear constraints. Some of the RBCC optimally constraints are mentioned in reference [7] but the applied constraint was chosen arbitrarily to show the effect of constraints existence. Boundary values of the variables were set as $7<X_1<21$; $4<X_2<16$ and $1<X_3<3$ and the relationship between isolator aspect ratio (L/D) to the ram burner and mixture inlet area ratio (A_8/A_5) was considered as a linear constraint. That is, $X_1 – 4X_3 > 0.0$.

3. 0 RESULTS AND DISCUSSIONS

3.1 Flow Field Overview

Color contours of Mach number, temperature and static pressure of the RBCC internal flow path are shown in Figure 2 for base case simulation (case 14). The rocket engine plumes are clearly visible in the middle of the RBCC ducts. The flow is generally two-dimensional between the rocket engine exit and the afterburner hydrogen injection. The Mach number contours indicate that the flow was entirely subsonic as it entered the diffuser section of the duct. The flow was not choked at the RBCC throat. The average duct nozzle exit Mach number was approximately 0.76.

Figure 3 shows the side wall static pressure comparison between the experimental data with the CFD simulation results. This comparison was done to validate the simulation. The predictions are generally good with slight underprediction close to the primary rocket exit.

3.5 Optimization results

The CFD data of 27 cases were used to generate a response surface (Table 3). This response surface was used for training the neural network and later it was used for objective function evaluation. A spreadsheet was used to evaluate the individual and total desirability/objective function.

After 63 iterations, system level converged to the optimum value**.** Figure 4 shows a convergence history of objective function and constraints. The value of the objective function jumps from one solution domain to another, as it tries to reduce the interdisciplinary discrepancies during the optimization process. Figure 5 shows the system level convergence of design variables.

4.0 CONCLUSIONS

For the range of A_s/A_p studied, the smallest primary thruster (A_s/A_p=15.66), pumped the most secondary flow. The A_s/A_p=15.66, configuration clearly had the highest by-pass ratio and best mixture thrust efficiency. Both L/D and A_8/A_5 had less dramatic but yet significant effects on by-pass ratio. For this configuration the rocket exit size was smallest (0.762 cm). Again, the mixing results primarily from the turbulent and viscous shear forces in steady flow ejectors. Increasing the interfacial shear area between the primary and secondary flows will increase the mixing action in terms of required length. And from this study it is noticeable that smaller primary rockets has proven effective in reducing the mixing length, which agree with the conceptual design of RBCC engine.

5.0 ACKNOWLEDGEMENT

This work has been supported by NASA Marshall Space Flight Center under grant No. NAG8-1644.

6.0 REFERENCES

1 Escher, William J. D. and B. J. Flomes: A Study of Composite Propulsion Systems For Advanced Launch Vehicle Application, Contract NAS7-377, The Marquardt Corporation, Van Nuys, California, 1966,Vol.1-7.

2. Wang, T.-S., Mc Connaughey, P., Warsi, *S.*, and Chen, Y.S., "Computational Pollutant Environment Assessment from Propulsion System Testing," Journal of Spacecraft and Rockets, Vol. 33, No.3, May-June 1996, pp.386-392.

3. Gordon, S., and McBride, B.J.," Compute Program for Calculation of Complex Chemical Equilibrium Compositions and Applications," NASA Ref. Pub. 1311, October 1994.

4. Sparks Jr., D.W., and Maghami, P. G.: Neural Networks for Rapid Design and Analysis, AIAA-98-1779.

5. Shyy, W., Tucker, Kevin P., and Vaidynathan, R., "Response Surface and Neural Network Techniques for Rocket Engine Injector Optimization," AIAA -99-2455, June 1999.

6. Gill, P. E., Murray, W., Saunders, M.A., and Wright, M. H.: User's Guide for NPSOL (Version 4.0) - A Fortran Package for Nonlinear Programming, Technical Report SOL 86-2, Jan. 1986, U.S.A

7. Eldred, C., Powd1, R., and Stanley, D "Single Stage Rocket Options for Future Launch Vehicles," AIAA Paper 93-4162, Sept. 1993.

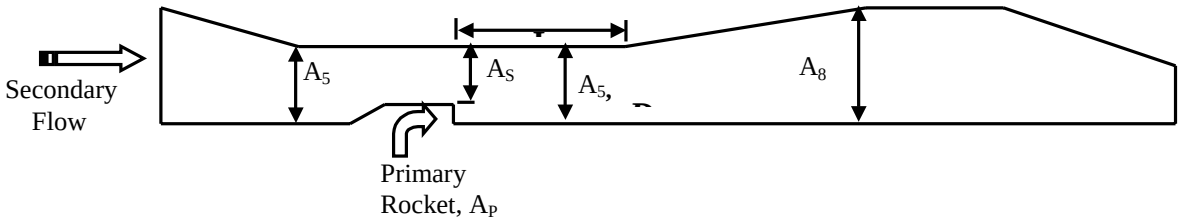

Figure 1: Schematic View of a 2-D Axissymetric RBCC Engine.

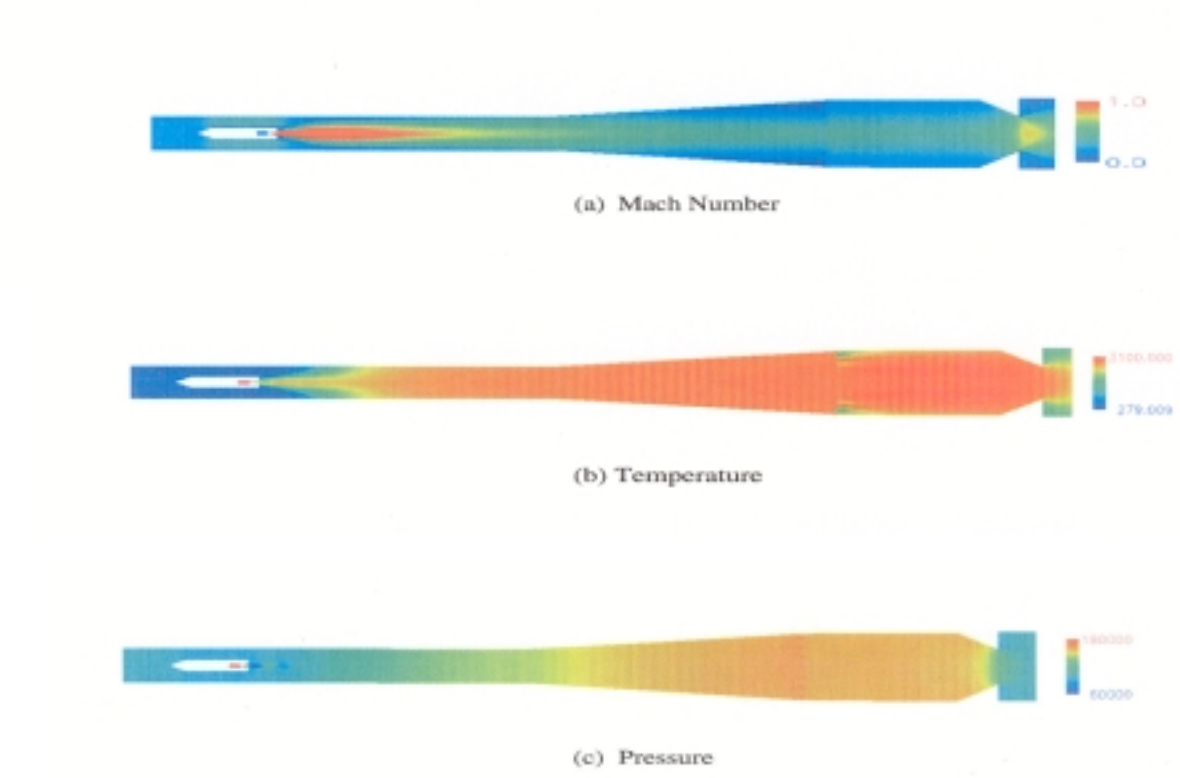

Figure 2. Calculated Mach Number, Temperature, and Static Pressure contour lines of RBCC Duct.

Table 1: RBCC Inlet/Ejector Design Trade Space

	L/D=7			L/D=14			L/D=21		
	As/Ap=4.5	As/Ap=7.3	As/Ap=15.6	As/Ap=4.5	As/Ap=7.3	As/Ap=15.6	As/Ap=4.5	As/Ap=7.3	As/Ap=15.6
A8/A5=1.0									x
A8/A5=1.5	x	x	x	x	x	x	x	x	x
A8/A5=2.0	x	x	x	x	x	x	x	x	x
A8/A5=2.5	x	x	x	x	x	x	x	x	x

Table 2: Primary Thruster Exit Conditions for Various Design Configuration.

Design Variables A_s/A_p	Chamber Pressure P_i (atm)	Exit Pressure P_e (atm)	Pressure Ratio P_i/P_e	Supersonic Area Ratio A_e/A_t	Velocity at Rocket Exit (m/s)	Temperature at Rocket Exit (K)
4.55	34.08	0.7	48.625	9	1289.7	1604.65
7.33	34.08	1.04	32.730	6	1338.0	1737.94
15.66	34.08	2.08	16.365	3	1422.7	1988.1

Table 3. Figures of Merit Results for the Inlet/Ejector Trade Study

Case No	L/D	As/Ap	A8/A5	By-pass Ratio	Ejector Compression Ratio	Mixer Thrust Efficiency	Desirability D1	Desirability D2	Desirability D3	Objective Function, D
1	7	4.55	1.5	1.749	1.158	0.352	0.312	0.158	0.529	3.370
2	7	4.55	2	2.211	1.119	0.550	0.428	0.119	0.707	3.030
3	7	4.55	2.5	2.368	1.190	0.393	0.467	0.190	0.571	2.703
4	7	7.33	1.5	2.523	1.239	0.360	0.506	0.239	0.538	2.487
5	7	7.33	2	3.092	1.162	0.545	0.648	0.162	0.704	2.382
6	7	7.33	2.5	3.399	1.253	0.425	0.725	0.253	0.601	2.087
7	7	15.66	1.5	4.050	1.310	1.100	0.888	0.310	1.000	1.538
8	7	15.66	2	5.449	1.235	0.628	1.237	0.235	0.766	1.650
9	7	15.66	2.5	5.888	1.321	0.720	1.347	0.321	0.830	1.407
10	14	4.55	1.5	1.670	1.152	0.394	0.293	0.152	0.571	3.400
11	14	4.55	2	1.900	1.096	0.318	0.350	0.096	0.492	3.925
12	14	4.55	2.5	1.926	1.132	0.323	0.357	0.132	0.498	3.493
13	14	7.33	1.5	3.827	1.224	0.432	0.832	0.224	0.608	2.066
14	14	7.33	2	4.116	1.149	0.378	0.904	0.149	0.556	2.374
15	14	7.33	2.5	4.495	1.184	0.351	0.999	0.184	0.528	2.176
16	14	15.66	1.5	3.758	1.308	0.761	0.814	0.308	0.857	1.670
17	14	15.66	2	4.643	1.272	0.917	1.036	0.272	0.953	1.550
18	14	15.66	2.5	4.946	1.250	1.269	1.111	0.250	1.000	1.532
19	21	4.55	1.5	1.728	1.137	0.240	0.307	0.137	0.395	3.915
20	21	4.55	2	2.114	1.144	0.321	0.403	0.144	0.496	3.265
21	21	4.55	2.5	2.250	1.136	0.268	0.438	0.136	0.432	3.393
22	21	7.33	1.5	2.398	1.226	0.987	0.475	0.226	0.993	2.110
23	21	7.33	2	3.691	1.206	0.512	0.798	0.206	0.677	2.081
24	21	7.33	2.5	3.870	1.185	0.429	0.842	0.185	0.604	2.197
25	21	15.66	1.5	3.841	1.294	2.712	0.835	0.294	1.000	1.596
26	21	15.66	2	5.933	1.295	0.761	1.358	0.295	0.857	1.427
27	21	15.66	2.5	6.857	1.277	0.470	1.589	0.277	0.641	1.524

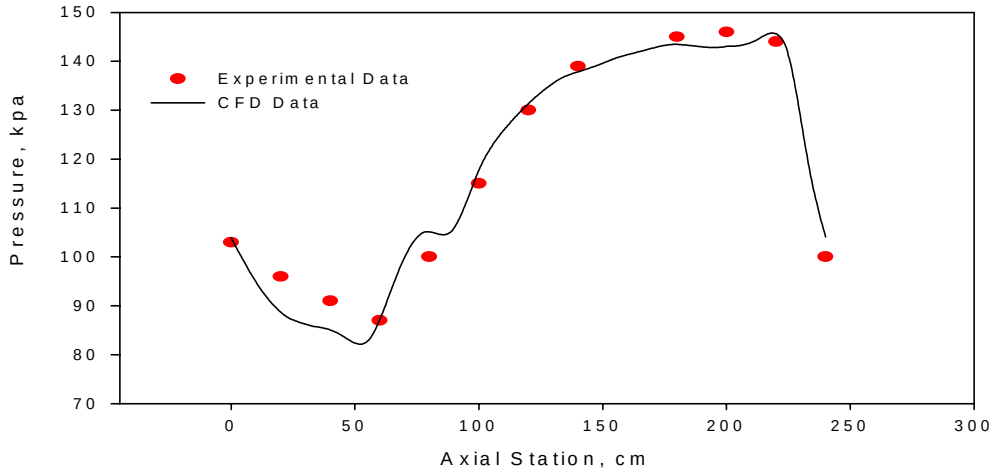

Figure 3. Static Pressure Comparison of CFD Simulation with Experimental Data.

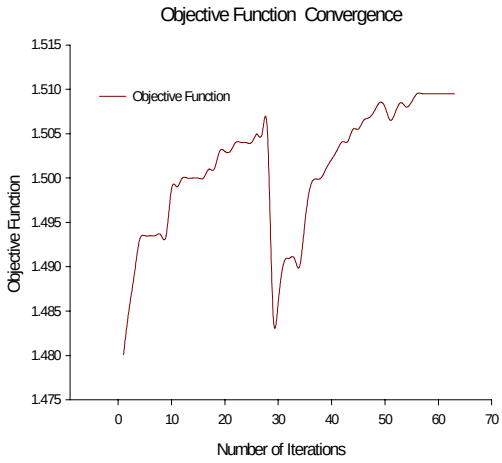

Figure 4. Convergence History of Objective Function

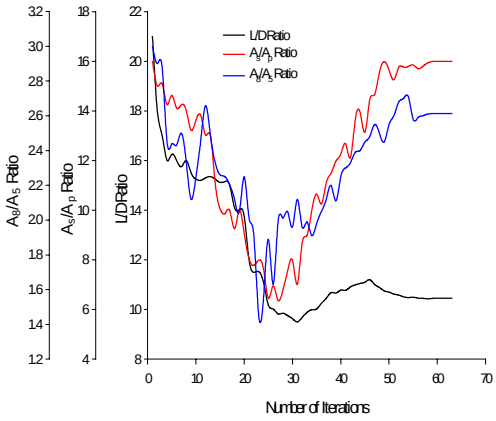

Figure 5. System Level Convergence of Design Variables